IOP Publishing Physica Scripta
Phys. Scr. 95 (2020) 035220 (13pp) https://doi.org/10.1088/1402-4896/ab46c9

Fractional symbolic network entropy analysis for the fractional-order chaotic systems

Shaobo He[1], Kehui Sun[1,3] and Xianming Wu[2]

[1] School of Physics and Electronics, Central South University, Changsha 410083, People's Republic of China
[2] School of Mechanical and Electrical Engineering, Guizhou Normal University, Guiyang 550025, People's Republic of China

E-mail: kehui@csu.edu.cn

Received 6 May 2019, revised 21 July 2019
Accepted for publication 23 September 2019
Published 6 February 2020

Abstract

Complexity analysis of fractional-order chaotic systems is an interesting topic of recent years. In this paper, the fractional symbolic network entropy measure algorithm is designed in which the symbol networks are built and fractional generalized information is introduced. Complexity of the fractional-order chaotic systems is analyzed. It shows that the proposed algorithm is effective for measure complexity of different pseudo random sequences. Complexity decreases with the decrease of derivative order in the fractional-order discrete chaotic system while changes with the derivative order in the fractional-order continuous chaotic system. Moreover, basin of attraction is also determined by the derivative order. It provides a basis for parameter choice of the fractional-order chaotic systems in the real applications.

Keywords: fractional calculus, complexity, fractional entropy, coexisting attractors

(Some figures may appear in colour only in the online journal)

1. Introduction

To observe complexity of non-natural and natural systems, the most direct way is to find some ways to analyze their nonlinear time series. There are many methods fulfill this target such as phase diagram, bifurcation diagram, 0–1 test [1], and complexity measure algorithms. Among those methods, measure complexity is a handy way since a reliable result can be obtained if a segment of time series is given. Until now, complexity of many different nonlinear time series has been investigated, such as EEG signal [2, 3], ECG signal [4–6], EMG signal [7], HRV signal [8], traffic signal [9], electricity signal [10], stock signal [11] and fault detection signal [12].

Currently, there are many different entropy and complexity measure algorithms for nonlinear time series, and they are designed from different point of view. Generally, those methods can be divided as time domain (TD) methods and frequency domain (FD) methods. TD methods measure complexity using the time series directly. In fact, most of the complexity measure algorithms belong to the TD method. FD methods are designed based on the frequency transformation. There are mainly three FD methods including C_0 complexity measure algorithm [13], the spectral entropy (SE) algorithm [14] and the Wavelet entropy (WE) algorithm [15]. Specifically, C_0 algorithm and SE algorithm estimate complexity based on the discrete Fourier transformation, while WE algorithm is proposed based on the Wavelet transformation. Moreover, according to different information theory, those complexity measure algorithms are divided as entropy measure algorithms [14–19], complexity estimation algorithms [20–22] and fractal dimension [23]. Generally, entropy methods are designed based on the Shannon entropy [24]. Currently, there are many different entropy estimation algorithms such as permutation entropy algorithm [17], SE [14], WE [15], Symbolic entropy [18] and network entropy [19].

[3] Author to whom any correspondence should be addressed.

Komologrov *et al* [25] discussed the concept of complexity in nonlinear time series. Later, Lempel and Ziv [20] proposed the famous Limpel–Ziv algorithm based on the concept. Strictly speaking, the exhaustive entropy [26], ApEn [27], SampEn [28] and FuzzyEn [29] are designed by combing the Komologrov complexity and Shannon information theory.

It is still an interesting topic to design new complexity measure algorithms for nonlinear time series. At present, designing network entropy algorithms has become a new research hotspot and some works have been reported. For instance, the horizontal visibility graphs [30–32] take into account the visibility of elements in a time series. But the size of the build network increase with the length of the time series. How to build a network from the chaotic time series and to design a related network entropy algorithm is still a task of great challenge. Meanwhile, Machado [33] proposed the concept of fractional generalized information theory which is the modification of the Shannon entropy. He *et al* [34] designed the fractional FuzzyEn algorithm and applied it to measure complexity of EEG signals from normal health persons and epileptic patients. Xu *et al* [35] proposed the weighted fractional permutation entropy and fractional sample entropy and analyzed nonlinear Potts financial dynamics. In this work, we focus on the designing a fractional network entropy method with limited size of network.

Until now, complexity in the chaotic systems has aroused the concern of scholars. Grassberger *et al* [22] estimated the Kolmogorov entropy of a chaotic signal, Liu *et al* [36] analyzed complexity chaotic binary sequences, Li *et al* [37] calculated information flow between two chaotic semiconductor lasers be employing the symbolic transfer entropy, He *et al* [38] estimated complexity of chaotic systems based on different algorithms, Rondoni *et al* [39] investigated the optical complexity in the external cavity semiconductor laser chaotic system, and Natiq *et al* [40] analyzed dynamics and complexity of a new 4D chaotic Laser system. Meanwhile, designing more complex chaotic systems and its stability analysis aroused interests of researchers [41, 42]. For example, Stenflo [43] proposed a generalized Lorenz equations for acoustic-gravity waves. In real applications, we call this system as the Lorenz–Stenflo system. Then complexity in the Lorenz–Stenflo system and the fractional-order Lorenz–Stenflo system is investigated [44–46]. For instance, Wang *et al* [46] investigated complex dynamics of fractional-order Lorenz-Stenflo system. There are two kinds of fractional-order chaotic systems. One kind is the fractional-order discrete time chaotic system and the other is the fractional-order discrete time chaotic system. Complexity in the fractional-order chaotic systems deserves further research, especially to investigate how complexity changes with the derivative order.

The rest of this paper is organized as follows. In section 2, two fractional-order chaotic systems are presented and some questions regarding this study are introduced briefly. In section 3, the symbolic networks of chaotic systems are built, and the fractional symbolic network entropy (FSNE) algorithm is proposed. In section 4, complexity of different fractional-order chaotic systems is analyzed. Finally, the results are summarized.

2. Systems and the existing questions

At present, dynamics in the fractional-order discrete chaotic map and multistability in the fractional-order continuous chaotic system aroused interests of researchers [47]. In this section, the fractional 2D Sine ICMIC modulation map [48] and the fractional-order Li's system [49] with multistability are chosen as the representatives of the fractional-order systems. Moreover, we state the main targets of this paper briefly.

2.1. Fractional-order chaotic systems

Recently, Liu *et al* [48] proposed a 2D Sine ICMIC modulation map (2D-SIMM), which is defined by

$$\begin{cases} x_1(i) = a\sin(\omega x_2(i-1))\sin(b/x_1(i-1)) \\ x_2(i) = a\sin(\omega x_1(i))\sin(b/x_2(i-1)) \end{cases}, \tag{1}$$

where a, b and ω are the system parameters, and a, b, $\omega \in (0, +\infty)$. By introducing the fractional difference of Caputo sense [50] to the system, the fractional-order 2D-SIMM

$$\begin{cases} {}^{C}\Delta_{t_0}^{q} x(i) = a\sin(\omega y(i+q-1))\sin(b/x(i+q-1)) - x(i+q-1) \\ {}^{C}\Delta_{t_0}^{q} y(i) = a\sin(\omega x(i+q))\sin(b/y(i+q-1)) - y(i+q-1) \end{cases}, \tag{2}$$

where $q \in (0, 1]$ is the fractional derivative order. The numerical solution of this system is given by

$$\begin{cases} x(i) = x(0) + \sum_{j=1}^{n} \frac{\Gamma(i-j+q)}{\Gamma(q)\Gamma(i-j+q)}\left[a\sin(\omega y(j-1))\sin\left(\frac{b}{x(j-1)}\right) - x(j-1)\right] \\ y(i) = y(0) + \frac{\Gamma(i-j+q)}{\Gamma(q)\Gamma(i-j+q)}\left[a\sin(\omega x(j))\sin\left(\frac{b}{y(j-1)}\right) - y(j-1)\right] \end{cases}, \tag{3}$$

here, $\Gamma(\cdot)$ is the gamma function. Let $a = 2$, $b = 3$ and $\omega = \pi$, and phase diagrams with different order q are shown in figure 1. It shows that the phase diagrams become fuzzier

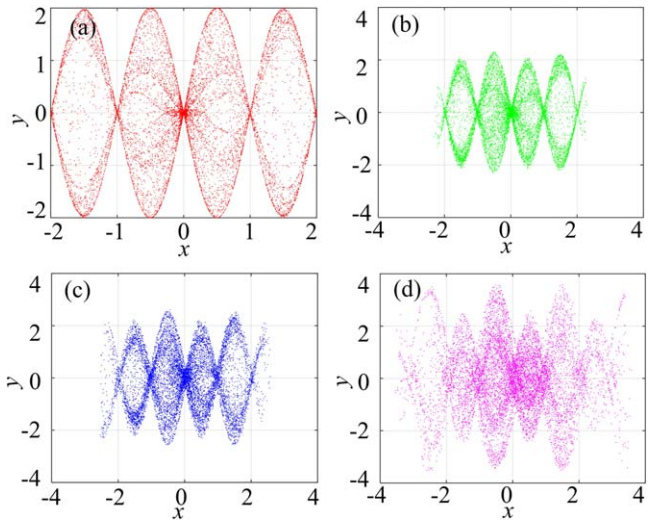

Figure 1. Phase diagrams of the fractional 2D-SIMM with different derivative order q (a) $q = 1$; (b) $q = 0.9$; (c) $q = 0.8$; (d) $q = 0.5$.

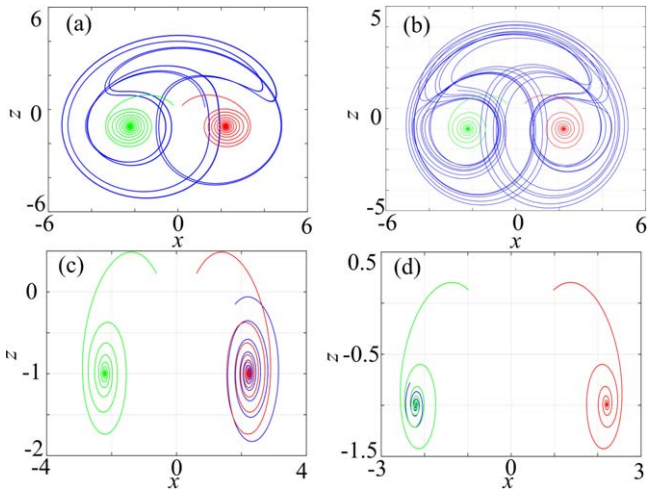

Figure 2. Coexisting attractors in the fractional-order Li system with different derivative order q (a) $q = 0.99$; (b) $q = 0.98$; (c) $q = 0.97$; (d) $q = 0.95$.

with the decrease of derivative order q due to increase of memory effect.

Li *et al* [49] investigated a new three dimensional system of first-order autonomous, ordinary differential equations, which is defined as

$$\begin{cases} \dot{x} = y + yz \\ \dot{y} = -xz + yz \\ \dot{z} = -\varepsilon z - xy + \beta \end{cases}, \tag{4}$$

where ε and β are the system parameters. Coexisting point attractors and limit cycles are observed in this system in a relatively large region of parameter space with different initial conditions. In this study, the Caputo fractional derivative is introduced and its corresponding fractional-order counterpart is

$$\begin{cases} D_{t_0}^q x = y + yz \\ D_{t_0}^q y = -xz + yz \\ D_{t_0}^q z = -\varepsilon z - xy + \beta \end{cases}. \tag{5}$$

Here $q \in (0, 1]$. The system is solved by employing the predictor-corrector algorithm. Specifically, the *fde12.m* function by Garrappa[4], which is a Matlab realization of the predictor-corrector algorithm, is used in this paper.

Let $\varepsilon = 0.9$, $\beta = 4$ and step size of time be 0.01. The coexisting phase projections of the system are sown in figure 2. It shows the three coexisting attractors for $q = 0.99$ and 0.98. Then two coexisting attractors are observed for $q = 0.97$ and $q = 0.95$ since attractor with initial condition given by $[x_0, y_0, z_0] = [-5.4, -7.4, -1]$ overlaps with other attractors. Moreover, basins of attraction of system (5) with different derivative q are illustrated in figure 3, where $z_0 = -1$, x_0 and y_0 vary from -10 to 10 with step size of 0.2. It shows that the two basin of attraction plots are different. When $q = 0.98$, different states are mixed, while the basin of attraction for $q = 0.99$ has clearer boundaries. Thus it indicates that the derivative order changes the dynamics of the system and affects the coexisting attractors as well.

Here, suppose that the obtained nonlinear time series is defined as $\{x(n), n = 0, 1, 2,\cdots, N-1\}$, and it is discretized quantitative time series of θ bits, and it is denoted as $\{s(n), n = 0, 1, 2,\cdots, N-1\}$. Thus $s(n)$ has 2^θ possible symbols. For instance, when $\theta = 8$, there are 256 possible symbols in the series of $s(n)$. In this paper, two different quantization methods are considered to discrete the time series to θ bits.

Method one: The time series is divided as 2^θ parts by employing the following method

$$s(n) = \begin{cases} 0, & \text{if} \quad \min(x) \leqslant x(n) < \Delta x \\ 1, & \text{if} \quad \Delta x \leqslant x(n) < 2\Delta x \\ \vdots & \\ 2^\theta - 1, & \text{if} \quad (2^\theta - 1)\Delta x \leqslant x(n) \leqslant \max(x) \end{cases}. \tag{6}$$

Method two: It is designed by performing the following steps.

Firstly, convert the original time series $\{x(n), n = 0, 1, 2,\cdots, N-1\}$ to an integer number sequence as

$$\varphi(n) = \text{round}(x(n) \times 10^w), \tag{7}$$

in which $n = 0, 1, 2,..., N-1$ and w is the control parameter. Here, in this paper, $w = 10$.

Secondly, express each $\varphi(n)$ as a binary number by

$$\varphi(n) = DB_{63}DB_{62} \cdots DB_1DB_0. \tag{8}$$

Thirdly, the pseudo-random sequence $s(n)$ is obtained by

$$s(n) = DB_\theta \cdots DB_1DB_0, \tag{9}$$

where the first θ bits number are chosen to form a new number.

Fix $\theta = 8$, two segments of time series from system (2) and system (5) are converted to the pseudo-random sequences. The two quantization algorithms are used and results are illustrated in figure 4. Figures 4(a) and (d) show the original time series, while figures 4(b) and (e) present the pseudo-random sequences using method one and figures 4(c) and (f)

[4] https://mathworks.com/matlabcentral/fileexchange/32918-predictor-corrector-pece-method-for-fractional-differential-equations.

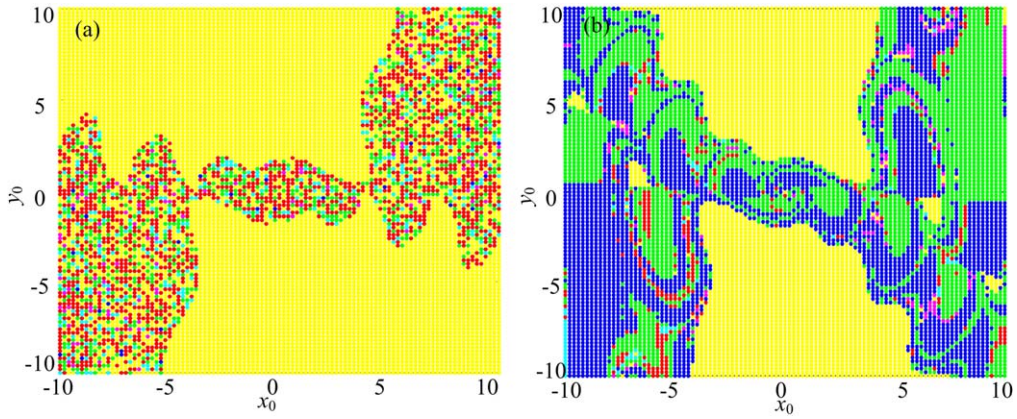

Figure 3. The basin of attraction of the fractional-order Li system with different derivative order q (a) $q = 0.98$; (b) $q = 0.99$.

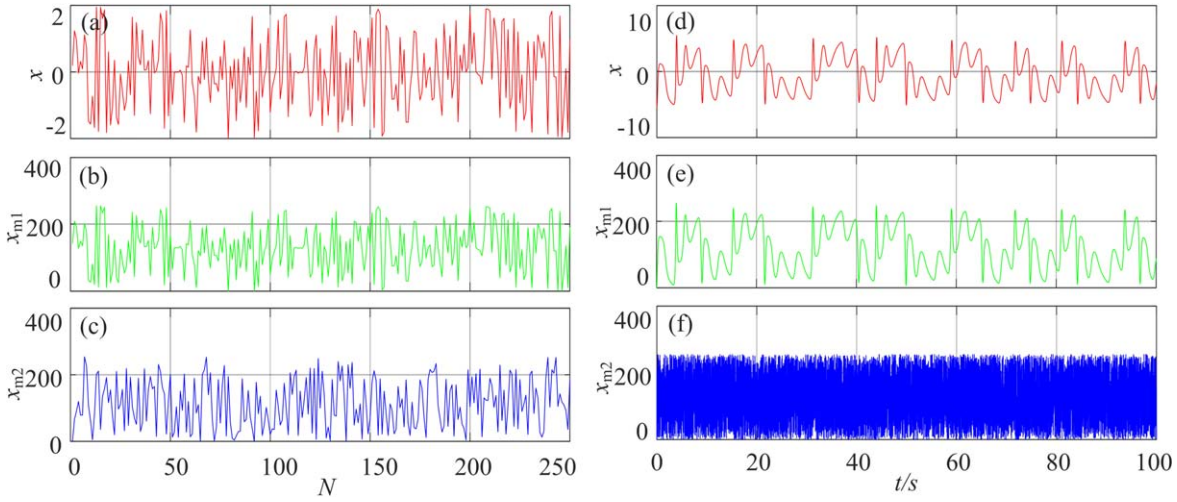

Figure 4. Time series of the fractional-order chaotic systems (a) original time series, (b) pseudo-random sequences using method one and (c) pseudo-random sequences using method two of the fractional 2D Sine ICMIC modulation map; (d) original time series, (e) pseudo-random sequences using method one and (f) pseudo-random sequences using method two of the fractional-order Li system.

present the pseudo-random sequences using method two. It shows that the fluctuation of pseudo-random sequences using method one is similar to the original time series, but pseudo-random sequences using method two is not. The main reason is that those pseudo-random sequences using method one keep more features of the original system.

2.2. Proposition of the questions

As mentioned above, it is an interesting topic to analyze complexity of factional-order chaotic systems, especially those systems with coexisting attractors. Meanwhile, there are still many issues should be discussed, which we expand as follows:

(1) The obtained chaotic pseudo-random sequence is a kind of stochastic signal. What is the relationship between complexity and randomness? Can pseudo-random sequence only be generated by the high complexity chaotic time series?
(2) Obviously, for a given chaotic time series, different quantization algorithms generate different pseudo-random sequences. How do the quantization algorithms affect the complexity measure results?
(3) There are some coexisting attractors in the fractional-order continuous chaotic systems which can be detected using the basins of attraction plots. Since the system has different kinds of basin of attraction and even different kinds of attractors, is it possible to identify coexisting attractors by employing the complexity measure algorithms?
(4) As it is well known that the fractional derivative order can be treated as a bifurcation parameter. How does complexity of such systems change with the decrease of derivative order?

3. Complexity analysis methods

3.1. Building the symbol networks

For a given θ-bit pseudo-random sequence $s(n)$, $n = 1, 2, \cdots, N$, we construct the following adjacent matrix

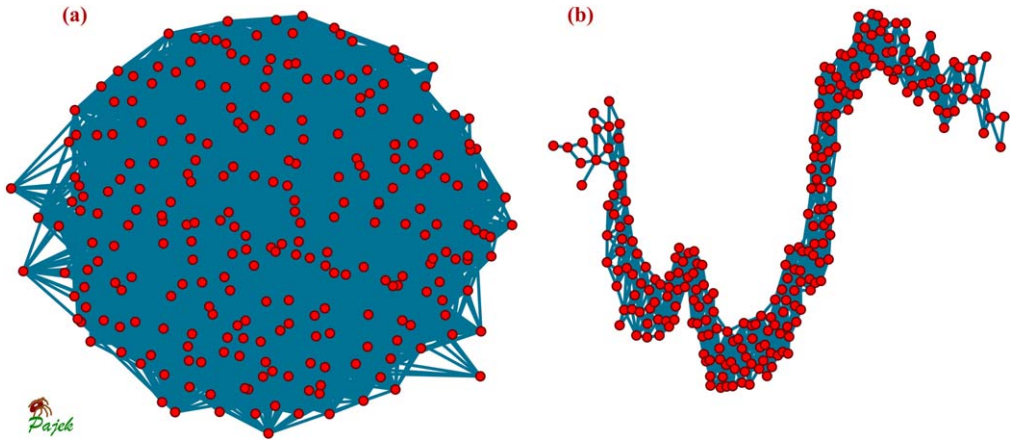

Figure 5. Networks of fractional-order chaotic systems using method one (a) fractional-order discrete chaotic map; (b) fractional-order continuous chaotic system.

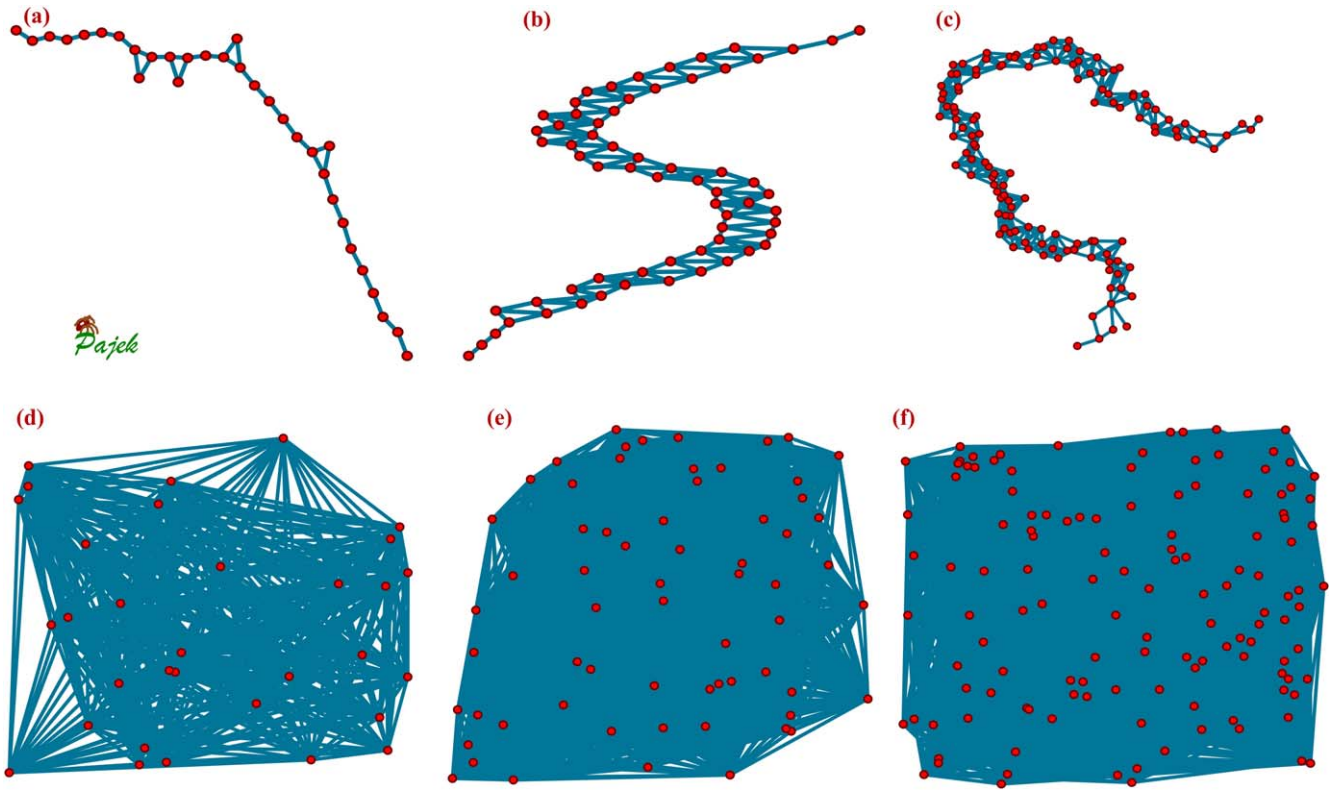

Figure 6. Networks of fractional-order continuous chaotic system (a) method one, $\theta = 5$; (b) method one, $\theta = 6$; (c) method one, $\theta = 7$; (d) method two, $\theta = 5$; (e) method two, $\theta = 6$; (f) method two, $\theta = 7$.

$M = \varphi_{i,j}$ $(i, j = 0, 1, \cdots, 2^{\theta} - 1)$ and the steps are given as follows.

Step 1: Let $k = 1$, $\varphi_{i,j} = 0$ $(i, j = 0, 1, \cdots, 2^{\theta} - 1)$.

Step 2: Check the change between $s(k - 1)$ and $s(k)$. If $s(k - 1) = m$ and $s(k) = n$, $(0 \leqslant m, n < 2^{\theta})$, then set values of $\varphi_{m,n}$ and $\varphi_{n,m}$ as one. After this, let $k = k + 1$.

Step 3: Repeat the Step 2 until $k = N - 1$. Thus we get a directed adjacent matrix which holds relationship between different symbols.

Two symbol $i - 1$ and $j - 1$ are connected if $\varphi_{i,j} \neq 0$, where the weight between the two nodes is the value of $\varphi_{i,j}$. Let $\theta = 8$, and time series as shown in figures 4(a) and (d) are used to build the symbolic networks. Figure 5 illustrates the symbolic networks of fractional-order chaotic systems, where the quantization method is method one. It shows that two networks are different due to the difference of system dynamics. The built network from the discrete map is more complex than that from the continuous system. Moreover, networks of fractional-order continuous chaotic system are drawn in figure 6, where two methods are used and $\theta = 3$, 4 and 5, respectively. Compared with method one, method two generates more complex networks as shown in figure 6. It

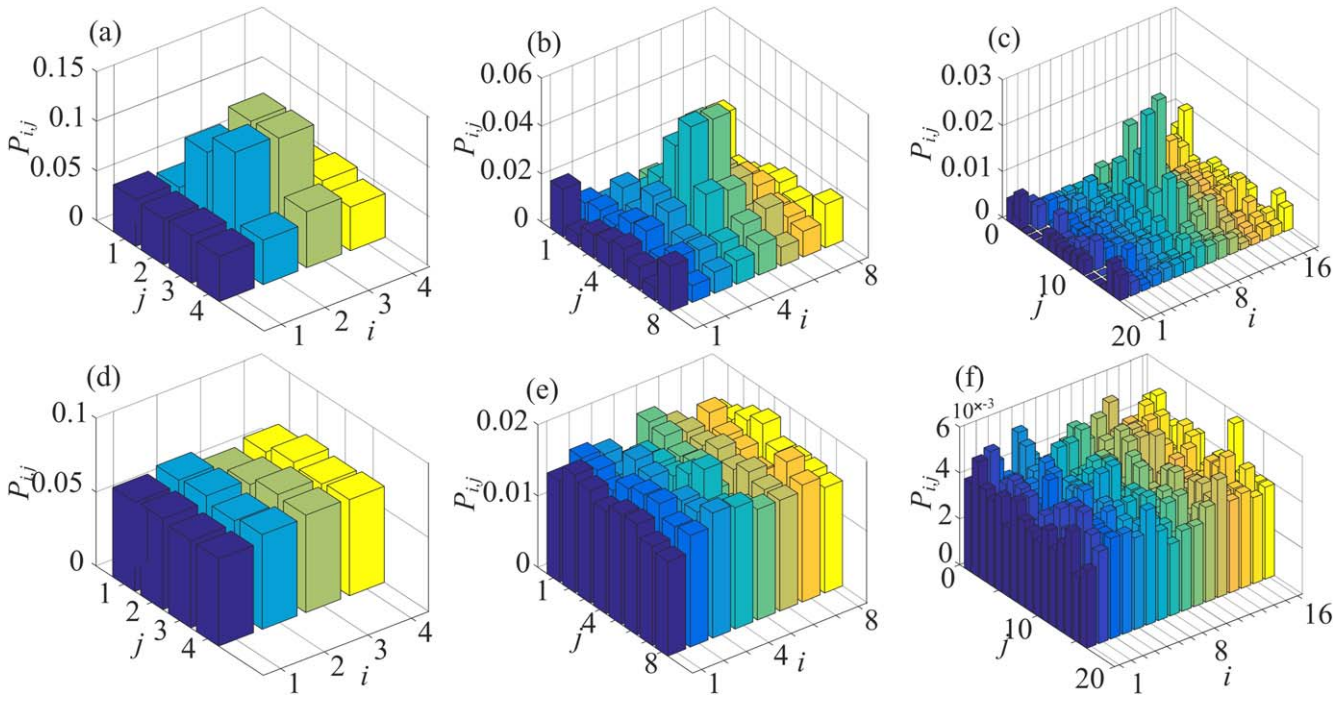

Figure 7. Probability distribution of the fractional-order discrete map (a) 2-bit case using method one; (b) 3-bit case using method one; (c) 4-bit case using method one; (d) 2-bit case using method two; (e) 3-bit case using method two; (f) 4-bit case using method two.

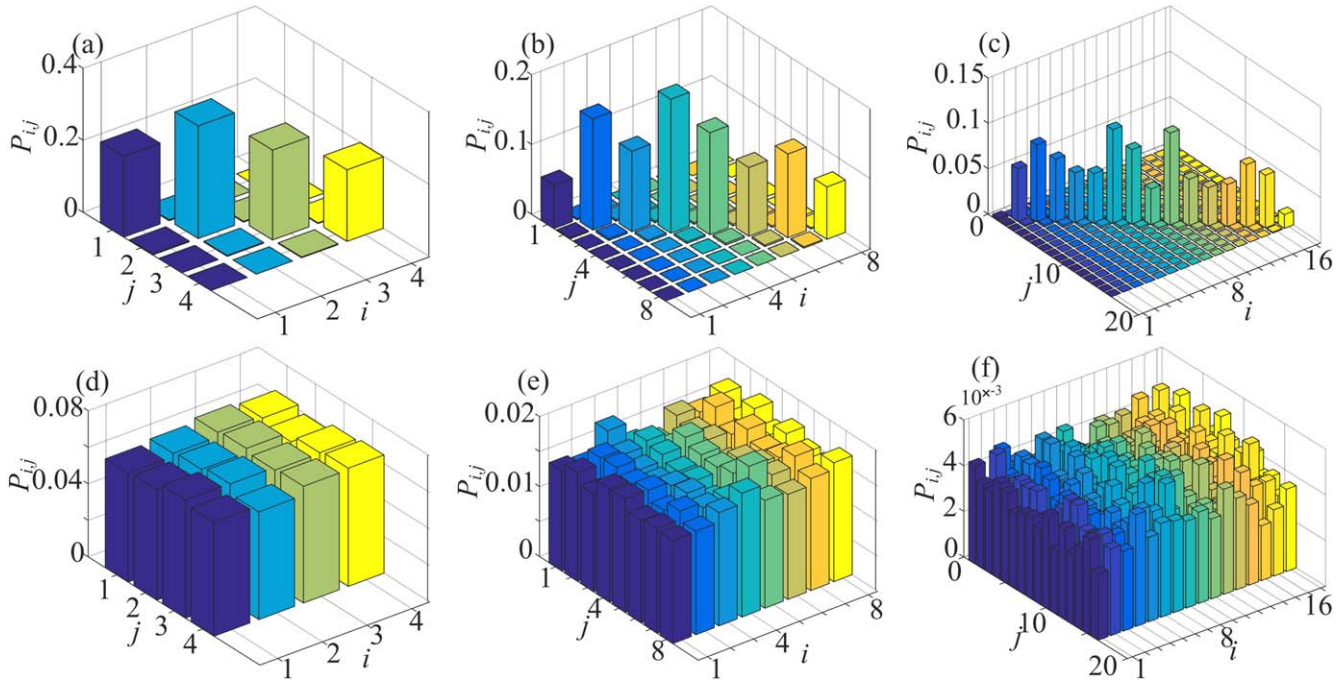

Figure 8. Probability distribution of the fractional-order continuous chaotic system (a) 2-bit case using method one; (b) 3-bit case using method one; (c) 4-bit case using method one; (d) 2-bit case using method two; (e) 3-bit case using method two; (f) 4-bit case using method two.

should be noted that those built networks are weighted and directed, and drawn by the Pajek software.

3.2. Extracting the probability distributions

To obtain the probability distributions from the network, we need to calculate the weights between each symbol. Let the weights matrix be defined as $M = \phi_{i,j}$ $(i, j = 0, 1, \cdots, 2^{\theta} - 1)$. Check the two symbols $s(k-1)$ and $s(k)$. If $s(k-1) = m$ and $s(k) = n$, $(0 \leqslant m, n < 2^{\theta})$, then value of $\phi_{m,n}$ increase one. Based on the weight matrix, the probability distribution is obtained. For the given θ-bit pseudo-random sequence $\{s(n), n = 1, 2, \cdots, N\}$, there are $N - 1$ times for counting the number of $\phi_{i,j}$. Thus the

two-dimensional probability distribution is denoted as

$$P_{i,j} = \frac{\phi_{i,j}}{N-1}. \tag{10}$$

Obviously, if $P_{i,j} = 0$, there is no connection between the symbol $i-1$ and the symbol $j-1$. However, since the symbolical visibility graph is bidirectional, the next symbol of symbol $j-1$ could be the symbol $i-1$ if $P_{j,i} \neq 0$, and the possibility depends on the value of $P_{j,i}$. Moreover, the idea situation is $P_{i,j} = \frac{1}{2^{2\theta}}$ $(i, j = 0, 1, \cdots, 2^{\theta} - 1)$, which means that the targeting time series is totally random in this case.

Probability distribution plots for two segments of time series as given in figures 4(a) and (d) are shown in figures 7 and 8, respectively. Here, the original time series are quantized as 5-bit, 6-bit and 7-bit pseudo-random sequences using the two methods. It shows in figures 7 and 8 that probability distribution plots are different for different systems when the method one is used. Those probability distribution plots based on method one carry characteristics of the original systems. The main reason is that the pseudo-random sequences have the similar fluctuation as the original time series, which are verified in figures 4, 5 and 6. Moreover, a comparison between figures 7(d)–(f) and 8(d)–(f) is carried out. The uniform probability distributions are observed for different time series, thus the characteristics of the original systems are lost. Therefore, how to choose a proper quantization algorithm should be discussed further, which will be carried out in the next section.

3.3. The FSNE algorithm

Recently a generalized expression of Shannon entropy is proposed by considering the fractional calculus, and it is defined by [33]

$$S_{\alpha} = \sum_{i} p_i \left\{ \frac{p_i^{-\alpha}}{\Gamma(\alpha+1)} [\ln p_i + \psi(1) - \psi(1-\alpha)] \right\}, \tag{11}$$

where α is the fractional order, and $\Gamma(\cdot)$ and $\psi(\cdot)$ represent the gamma and digamma functions, respectively. Moreover, the fractional-order information of is denoted as [20]

$$I_{\alpha} = \frac{p_i^{-\alpha}}{\Gamma(\alpha+1)} [\ln p_i + \psi(1) - \psi(1-\alpha)], \tag{12}$$

where $I_{\alpha} = 0$ if $p_i = 0$. Since we have the probability distribution of time series, the entropy can be calculated. By introducing the fractional Shannon entropy, the FSNE is defined by

$$\begin{aligned} \mathrm{FSNE}(s, \alpha) &= -\log(2^{2\theta}) \\ &\times \sum_{i,j=1}^{2^{\theta}} p_{i,j} \left\{ \frac{p_{i,j}^{-\alpha}}{\Gamma(\alpha+1)} [\log(p_{i,j}) + \psi(1) - \psi(1-\alpha)] \right\}. \end{aligned} \tag{13}$$

In the real estimation, α takes values between -0.4 and 0.5 [33, 34].

In this study, the coarse-grain process is introduced for complexity estimation of the continuous chaotic system. Thus FSNE for continuous chaotic systems is calculated based on the following two steps.

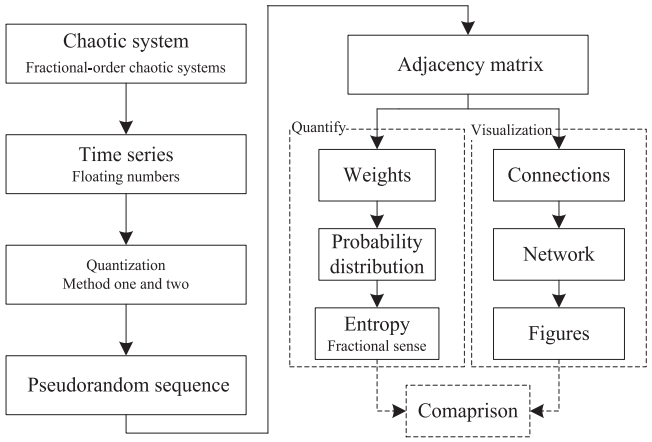

Figure 9. The schematic for complexity analysis of fractional-order chaotic systems.

Step 1: The coarse-grain process. For a given continuous time series $\{x(i): i = 1, 2, \cdots, N\}$, the coarse-graining time series is obtained by [51]

$$y^{\tau}(j) = \frac{1}{\tau} \sum_{i=(j-1)\tau+1}^{j\tau} x(i), \tag{14}$$

where $1 \leqslant j \leqslant \lfloor N/\tau \rfloor$, τ is the scale factor, and $\lfloor \cdot \rfloor$ is the floor function.

Step 2: Estimation of entropy. FSNE for the fractional-order continuous chaotic system is defined by

$$\mathrm{FSNE}(s, \alpha) = \sum_{\tau=1}^{10} 0.1\mathrm{FTDE}(y^{\tau}, \alpha). \tag{15}$$

Figure 9 shows the schematic for complexity analysis of fractional-order chaotic systems. Firstly, we need to solve the chosen fractional-order chaotic system and to quantize the obtained time series as pseudorandom sequence. Secondly, the adjacency matrix is obtained. Then, the probability distribution is extracted and its network is built. Finally, the FSNE can be estimated based on the probability distribution. Obviously, to estimate FSNE of the fractional-order chaotic system, we just need to capture a segment of time series from the system. Thus the proposed method can be employed to analyze complexity of different chaotic systems even with a higher dimension.

4. Complexity analysis of fractional-order chaotic systems

4.1. Effectiveness of FSNE

In this section, complexity of different chaotic systems versus system parameters is analyzed to verify the effectiveness of the proposed complexity measure algorithm.

For the discrete chaotic systems, 2D-SIMM and Logistic map are chosen, where 2D-SIMM is defined in equation (1) and the Logistic map is denoted as

$$x(n+1) = \mu x(n)(1 - x(n)), \tag{16}$$

where μ is the bifurcation parameter.

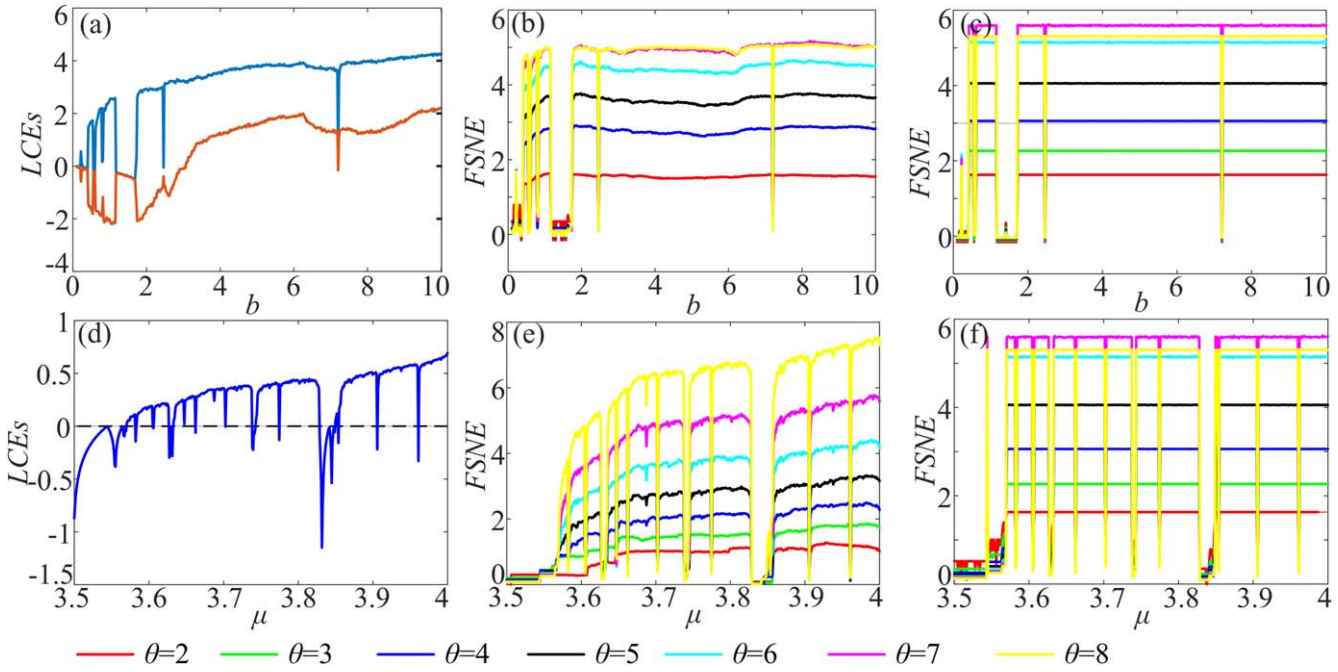

Figure 10. Dynamics and complexity of the discrete chaotic systems (a) LCEs of 2D-SIMM; (b) FSNE of 2D-SIMM based on method one; (c) FSNE of 2D-SIMM based on method two; (d) LCEs of Logistic map; (b) FSNE of Logistic map based on method one; (c) FSNE of Logistic map based on method two.

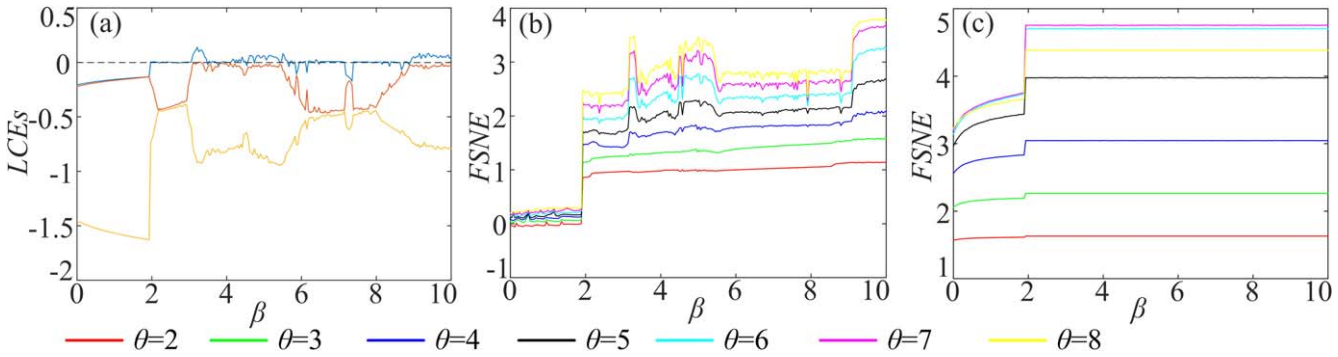

Figure 11. Dynamics and complexity of the fractional-order continuous chaotic system (a) LCEs; (b) FSNE based on method one; (c) FSNE based on method two.

Parameter b in the 2D-SIMM varies from 0.1 to 10 with step size of 0.0198 and parameter μ increases from 3.5 to 4 with an increment of 0.0001. Dynamics and complexity analyses results of these two discrete chaotic systems are illustrated in figure 10. Moreover, figure 11 shows the analysis results of the fractional-order continuous chaotic systems, where parameter β varies from 0 to 10 with step size of 0.02. Here, the conclusions are put forward in two aspects.

(1) The effectiveness of designed FSNE measure algorithm is verified. It shows in figures 10 and 11 that the FSNE analysis results based on method one agree well with LCEs analysis results, while that based on method two indicate that chaotic state has high complexity and non-chaotic state has low complexity. Meanwhile, complexity analysis result based on 8-bit pseudo-random sequence is the most satisfying as shown in figures 10 and 11.

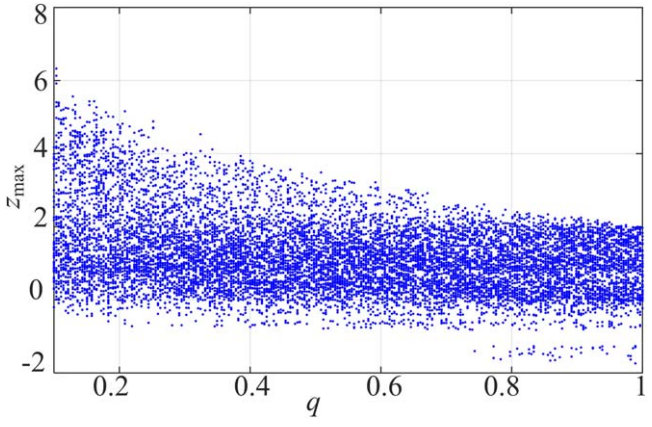

Figure 12. Bifurcation diagram of the fractional-order 2D-SIMM with the variation of derivative order q.

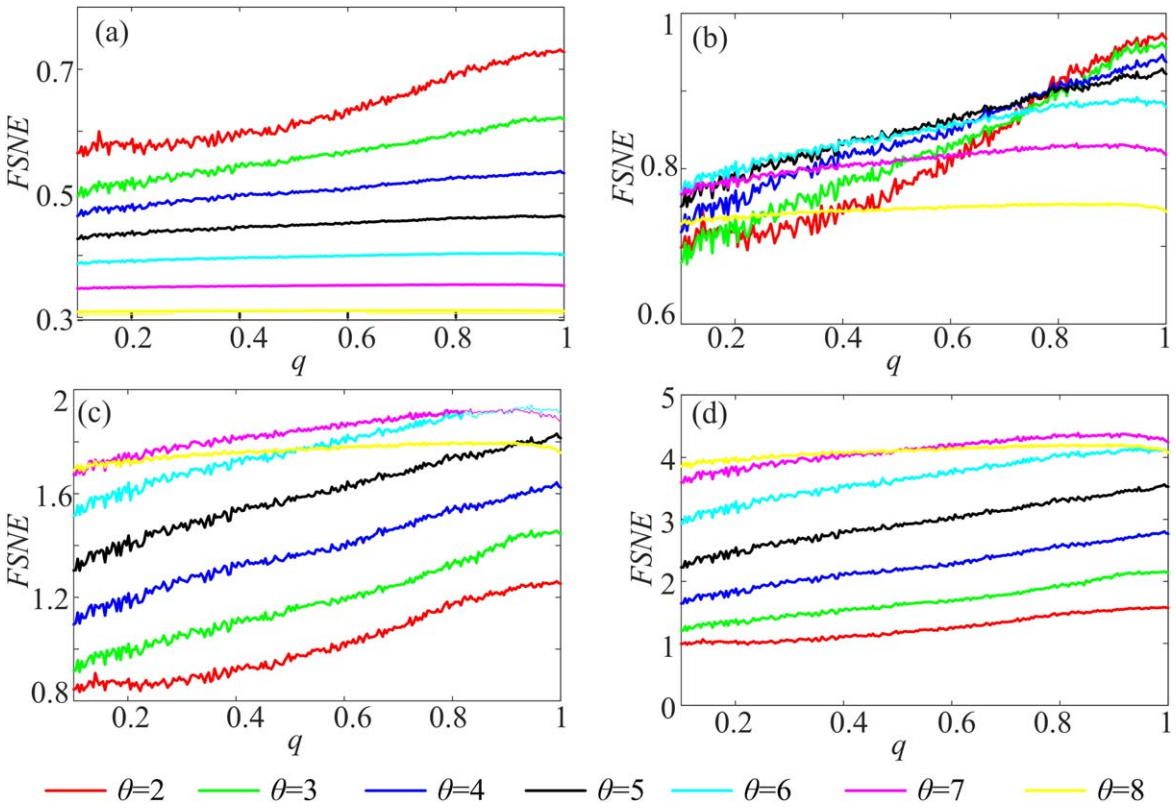

Figure 13. Complexity analysis results of the fractional-order 2D-SIMM with derivative order q (a) $\alpha = -0.1$; (b) $\alpha = 0.0$; (c) $\alpha = 0.1$; (d) $\alpha = 0.2$.

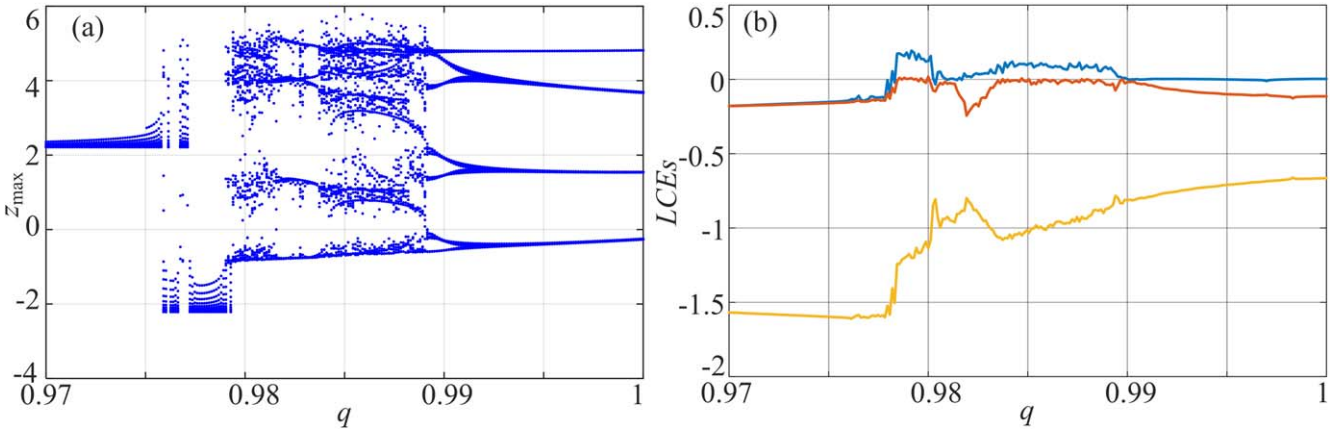

Figure 14. Dynamics analysis results of the fractional-order continuous chaotic system (a) bifurcation diagram; (b) LCEs.

(2) How to choose a proper quantization algorithm for different situation is confirmed. Since FSNE analysis results based on method one match the LCEs well, it can be used as an effective tool for dynamical analysis. However, FSNE analysis results based on method two indicate that pseudo-random sequences have the same high complexity if the original chaotic system is chaotic, and there are no difference between chaotic state and periodic state in the continuous chaotic systems as shown in figure 11. In fact, the method two has already been used to design the chaotic pseudo-random sequence generator for real applications [18, 52].

In conclusion, pseudo-random sequences based on method one can be used for complexity and dynamics analysis, but pseudo-random sequences based on method two can be used in the practical applications.

4.2. Complexity versus fractional order q

In this section, complexity versus fractional order q is analyzed, where the pseudo-random sequences based on the quantization method one are used.

Bifurcation diagram of the fractional-order 2D-SIMM with derivative order q varying is shown in figure 12, where the step size of q is 0.001. It shows that the system is chaotic for $q \in [0.1, 1]$. Meanwhile, the complexity analysis results are shown in figure 13, where the fractional order α in FSNE

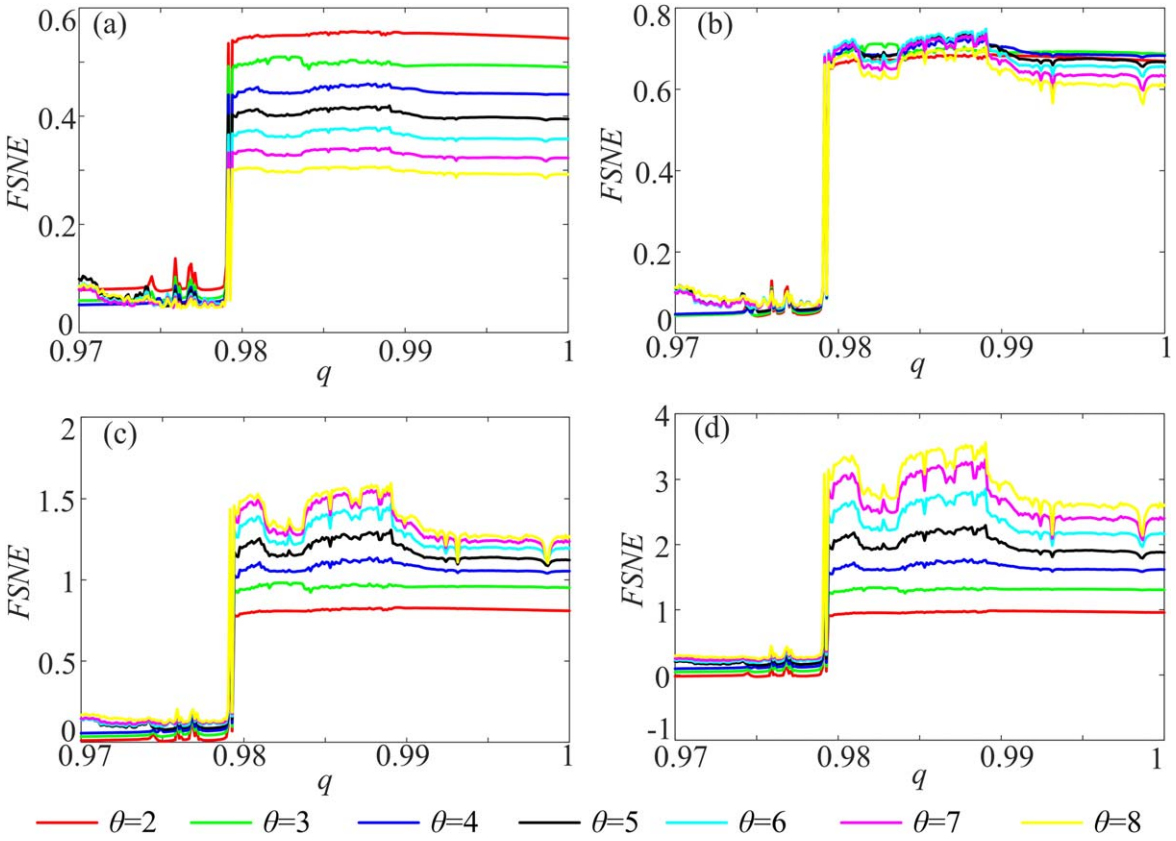

Figure 15. Complexity analysis results of the fractional-order continuous chaotic system with derivative order q (a) $\alpha = -0.1$; (b) $\alpha = 0.0$; (c) $\alpha = 0.1$; (d) $\alpha = 0.2$.

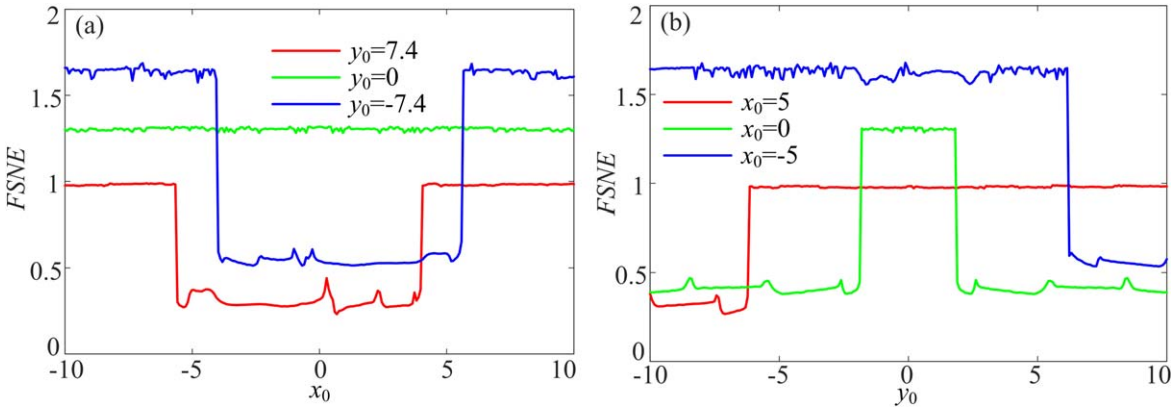

Figure 16. FSNE analysis result with the variation of initial conditions where $z_0 = -1$ (a) x_0 varying; (b) y_0 varying.

is given by -0.1, 0, 0.1 and 0.2. When $\alpha = 0$, the fractional generalized entropy is Shannon entropy, thus it shows that the Shannon entropy based analysis result cannot distinguish different cases. However, when α takes other values, different states are identified. Especially when $\alpha = -0.1$, complexity of different bits pseudo-random sequences are distinguished very well. Compared with Shannon entropy, fractional generalized entropy based entropy measure can obtain better analysis results. Moreover, it shows that complexity of the fractional-order 2D-SIMM increases with the increase of derivative order q.

Complexity of the fractional-order continuous chaotic system is analyzed by means of bifurcation diagram, LCEs and FSNE with different orders. As shown in figure 14, the system is periodic when q equals to one and near to one. Chaos is observed when q is smaller than 0.99. Rich dynamics are found in the fractional-order continuous chaotic systems. As shown in figure 15, FSNE has better measure result when the fractional order α takes values like -0.1, 0.1 and 0.2. For the fractional-order continuous chaotic system, FSNE with $\alpha = -0.1$ does not decrease when the system is periodic and the analysis results with $\alpha = 0.2$ agree with the

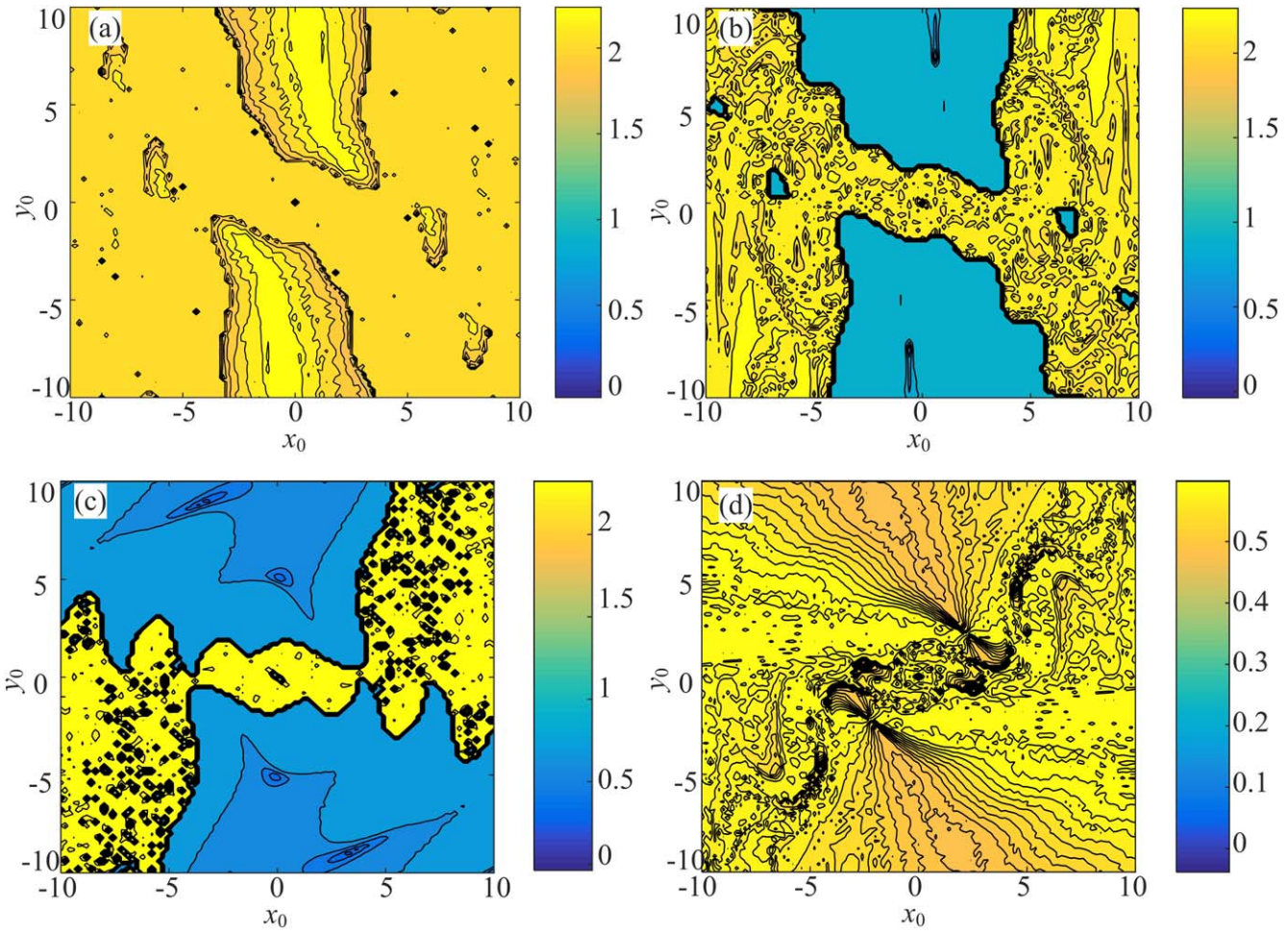

Figure 17. FSNE contour plots in the x_0−y_0 plane under different derivative order q (a) $q = 1$; (b) $q = 0.99$; (c) $q = 0.98$; (d) $q = 0.97$.

dynamical analysis results better. Obviously, the fractional-order system has higher complexity than its integer-order counterpart. Moreover, when $q < 0.98$, a higher complexity interval is observed. Thus in the fractional-order continuous chaotic system, complexity increases with the decrease of the derivative order q.

4.3. Complexity versus coexisting attractors

The fractional-order chaotic system has coexisting attractors, which means the system has different kinds of attractors with different initial conditions. The parameters of the system are $a = 0.9$ and $b = 4$. Pseudo-random sequences based on the quantization method one with eight bits for each symbol are used.

Let $z_0 = -1$, $y_0 = -7.4$, 0 and 7, and vary x_0 from -10 to 10 with step size of 0.025, complexity analysis results are shown in figure 16(a). When we fix $x_0 = -5$, 0 and 5 and vary y_0 with same step size, we obtain the complexity analysis results as shown in figure 16(b). It shows that complexity of the fractional-order continuous chaotic system changes with the initial conditions which means different coexisting attractors are detected by the FSNE measure algorithm.

Vary x_0 and y_0 between -10 and 10 with step size of 0.02, FSNE based contour plots in the initial condition x_0–y_0 plane are obtained as shown in figure 17, where $q = 1$, 0.99, 0.98 and 0.97. When $q = 1$, the system is solved by the 4th order Runge–Kutta algorithm. It also shows in figure 17 that complexity is different when the initial condition is different, which means the attractors of the system are different and coexisting attractors are observed. Comparing with figures 3(a) and (b), figures 17(b) and (c) have similar variation trends, respectively. Therefore, FSNE is an effective tool for analyzing coexisting in the fractional-order multistability chaotic systems. In addition, with the decrease of fractional derivative order q, the basin of attraction changes since FSNE complexity contour plots are different. When $q = 0.97$, there are significant changes in figure 17(d) comparing with other cases. The main reason is that the system with $q = 0.97$ is convergent according to figures 14 and 15, while the other cases are chaotic. Thus there are significant changes between figures 17(d) and (a)–(c). In brief, the basin of attraction changes with the derivative order q.

5. Discussion and conclusions

The FSNE measure algorithm is designed based on the fractional generalized entropy and the adjacent matrix. Complexity of fractional-order chaotic systems is analyzed

based on the proposed method. We answered the questions raised in section 2 in the manuscript, and the following discussion and conclusions which are also the answers of the questions are expanded as below.

(1) The proposed entropy measure algorithm is effective for complexity analysis of nonlinear time series. Compared with the normal Shannon entropy ($\alpha = 0$), fractional entropy (α takes other values) make the measure results better. Especially, when $\theta = 8$ and the method one are used, the analysis results agree well with the LCEs analysis results.
(2) Complexity measure results are affected by the quantization methods. Pseudorandom sequences based on method two have higher complexity than that based on the method one. When method one is used, complexity measure results have the similar trend as LCEs when the system parameters and the derivative order vary. However, complexity of the pseudorandom sequences based on method two does not change with the parameters and derivative order. It means that FSNE does not depend on the system parameters and derivative orders for those generated high complexity pseudorandom sequences. In other words, a pseudorandom sequence generator can be designed based on those chaotic systems with small complexity if the quantization method is effective.
(3) It shows that complexity of the fractional-order discrete chaotic system decrease with the decrease of derivative order, while complexity of the fractional-order continuous chaotic system changes with orders due to the different states. For the complexity of fractional-order continuous chaotic system, there are also other work to show this result although the solution algorithm is different. For instance, He *et al* [18, 52] show that complexity of fractional-order continuous chaotic systems increase with the decrease of derivative order when the system is solved by ADM and DTM.
(4) Complexity of the fractional-order continuous chaotic system is affected by the initial conditions. It means that dynamics of the system changes with the initial conditions. Therefore, coexisting attractors can be observed with different conditions. In fact, extreme multistability chaotic systems can have high complexity for real applications [53]. For these systems, the states could be different for different initial conditions.Thus we think that those extreme multistability chaotic systems provide better models for the pseudorandom number generations.
(5) Basin of attraction in both basin attraction plots and complexity contour plots of the fractional-order continuous chaotic system are different when the derivative order decreases. In fact, it is the first time we observe this phenomenon in the fractional-order chaotic system. It shows again that the dynamics of the fractional-order continuous chaotic system depends on the fractional derivative order q.

Acknowledgments

This work was supported by the China Postdoctoral Science Foundation (No. 2019M652791), the Postdoctoral Innovative Talents Support Program (No. BX20180386), the National Natural Science Foundation of China (Grant Nos. 11847159, 11747150, 61161006 and 61573383), the Natural Science Foundation of Hunan Province (Nos. 2019JJ5041, S2019JJSSLH0130).

References

[1] Gottwald G A and Melbourne I 2009 On the implementation of the 0–1 test for chaos *SIAM J. Appl. Dyn. Syst.* **8** 129–45
[2] Bandt C 2017 A new kind of permutation entropy used to classify sleep stages from invisible eeg microstructure *Entropy* **19** 197
[3] Lerga J, Saulig N and Mozetič V 2017 Algorithm based on the short-term rényi entropy and if estimation for noisy eeg signals analysis *Comput. Biol. Med.* **80** 1–13
[4] Kumar M, Pachori R B and Acharya U R 2018 Automated diagnosis of atrial fibrillation ecg signals using entropy features extracted from flexible analytic wavelet transform *Biocybernetics Biomed. Eng.* **38** 564–73
[5] Sayan M *et al* 2015 Can complexity decrease in congestive heart failure? *Physica* A **439** 93–102
[6] Voss A, Kurths J and Fiehring H 1992 Frequency domain analysis of highly amplified ecg on the basis of maximum entropy spectral estimation *Med. Biol. Eng. Comput.* **30** 277
[7] Dostál O *et al* 2018 Permutation entropy and signal energy increase the accuracy of neuropathic change detection in needle emg *Comput. Intell. Neurosci.* **2018** 5276161
[8] Udhayakumar R K, Karmakar C and Palaniswami M 2018 Understanding irregularity characteristics of short-term hrv signals using sample entropy profile *IEEE Trans. Biomed. Eng.* **65** 2569–79
[9] Du S, Mengjia X and Pengjian S 2017 Generalized sample entropy analysis for traffic signals based on similarity measure *Physica* A **474** 1–7
[10] Varotsos P A *et al* 2006 Entropy of seismic electric signals: analysis in natural time under time reversal *Phys. Rev.* E **73** 031114
[11] Yue W, Pengjian S and Yilong L 2018 Multiscale sample entropy and cross-sample entropy based on symbolic representation and similarity of stock markets *Commun. Nonlinear Sci. Numer. Simul.* **56** 49–61
[12] Jinde Z, Haiyang P and Junsheng C 2017 Rolling bearing fault detection and diagnosis based on composite multiscale fuzzy entropy and ensemble support vector machines *Mech. Syst. Sig. Process.* **85** 746–59
[13] Enhua S, Zhijie C and Fanji G 2005 Mathematical foundation of a new complexity measure *Appl. Math. Mech.* **26** 1188–96
[14] Ceravolo R, Lenticchia E and Miraglia G 2018 Use of spectral entropy for damage detection in masonry buildings in the presence of mild seismicity *Multidiscip. Digit. Publ. Inst. Proc.* **2** 432
[15] Rosso O A *et al* 2001 Wavelet entropy: a new tool for analysis of short duration brain electrical signals *J. Neurosci. Methods* **105** 65–75
[16] De Micco L *et al* 2012 Sampling period, statistical complexity, and chaotic attractors *Physica* A **391** 2564–75
[17] Bandt C and Pompe B 2002 Permutation entropy: a natural complexity measure for time series *Phys. Rev. Lett.* **88** 174102

[18] Shaobo H, Santo B and Bo Y 2018 Chaos and symbol complexity in a conformable fractional-order memcapacitor system *Complexity* **2018** 4140762

[19] Min L, Xingxing F and Gang W 2016 Network structure entropy and its dynamical evolution for recurrence networks from earthquake magnitude time series *Eur. Phys. J.* B **89** 131

[20] Lempel A and Ziv J 1976 On the complexity of finite sequences *IEEE Trans. Inf. Theory* **22** 75–81

[21] Feldman D P and Crutchfield J P 1998 Measures of statistical complexity: why? *Phys. Lett.* A **238** 244–52

[22] Grassberger P and Procaccia I 1983 Estimation of the kolmogorov entropy from a chaotic signal *Phys. Rev.* A **28** 2591

[23] Yosef A 1999 The use of generalized information dimension in measuring fractal dimension of time series *Physica* A **271** 427–47

[24] Claude Elwood S 1948 A mathematical theory of communication *Bell Syst. Tech. J.* **27** 379–423

[25] Kolmogorov A N 1965 Three approaches to the definition of the concept 'quantity of information' *Probl. Pereda. Inf.* **1** 3–11

[26] Mingku F *et al* 2007 Analysis on random-like property of chaotic motions with exhaustive entropy *2007 IEEE Int. Conf. on Automation and Logistics* (Piscataway, NJ: IEEE) pp 2420–5

[27] Pincus S 1995 Approximate entropy (apen) as a complexity measure *Chaos* **5** 110–7

[28] Richman J S and Moorman J R 2000 Physiological time-series analysis using approximate entropy and sample entropy *Am. J. Physiol.-Heart Circ. Physiol.* **278** H2039–49

[29] Weiting C *et al* 2009 Measuring complexity using fuzzyen, apen, and sampen *Med. Eng. Phys.* **31** 61–8

[30] Luque B *et al* 2009 Horizontal visibility graphs: exact results for random time series *Phys. Rev.* E **80** 046103

[31] Gutin G, Mansour T and Severini S 2011 A characterization of horizontal visibility graphs and combinatorics on words *Physica* A **390** 2421–8

[32] Zhongke G, Qing C and Yuxuan Y 2016 Multiscale limited penetrable horizontal visibility graph for analyzing nonlinear time series *Sci. Rep.* **6** 35622

[33] José M 2014 Fractional order generalized information *Entropy* **16** 2350–61

[34] Shaobo H, Kehui S and Rixing W 2018 Fractional fuzzy entropy algorithm and the complexity analysis for nonlinear time series *Eur. Phys. J. Spec. Top.* **227** 943–57

[35] Kaixuan X and Jun W 2017 Weighted fractional permutation entropy and fractional sample entropy for nonlinear potts financial dynamics *Phys. Lett.* A **381** 767–79

[36] Niansheng L 2011 Pseudo-randomness and complexity of binary sequences generated by the chaotic system *Commun. Nonlinear Sci. Numer. Simul.* **16** 761–8

[37] Nianqiang L *et al* 2012 Quantifying information flow between two chaotic semiconductor lasers using symbolic transfer entropy *Chin. Phys. Lett.* **29** 030502

[38] Shaobo H, Kehui S and Huihai W 2016 Multivariate permutation entropy and its application for complexity analysis of chaotic systems *Physica* A **461** 812–23

[39] Rondoni L *et al* 2017 Optical complexity in external cavity semiconductor laser *Opt. Commun.* **387** 257–66

[40] Hayder N, Said M, Al-Saidi N and Kilicman A 2019 Dynamics and complexity of a new 4d chaotic laser system *Entropy* **21** 34

[41] Dadras S *et al* 2017 A note on the lyapunov stability of fractional-order nonlinear systems *ASME 2017 Int. Design Engineering Technical Conf. and Computers and Information in Engineering Conf.* (American Society of Mechanical Engineers) V009T07A033

[42] Dadras S and Momeni H R 2009 A novel three-dimensional autonomous chaotic system generating two, three and four-scroll attractors *Phys. Lett.* A **373** 3637–42

[43] Stenflo L 1996 Generalized lorenz equations for acoustic-gravity waves in the atmosphere *Phys. Scr.* **53** 83–4

[44] Yu M Y and Yang B 1996 Periodic and chaotic solutions of the generalized lorenz equations *Phys. Scr.* **54** 140–2

[45] Pal S, Sahoo B and Poria S 2014 Multistable behaviour of coupled lorenz-stenflo systems *Phys. Scr.* **89** 045202

[46] Wang H, Kehui S and Shaobo H 2014 Dynamic analysis and implementation of a digital signal processor of a fractional-order lorenz-stenflo system based on the adomian decomposition method *Phys. Scr.* **90** 015206

[47] Munoz Pacheco J *et al* 2018 A new fractional-order chaotic system with different families of hidden and self-excited attractors *Entropy* **20** 564

[48] Wenhao L, Kehui S and Shaobo H 2017 Sf-simm high-dimensional hyperchaotic map and its performance analysis *Nonlinear Dyn.* **89** 2521–32

[49] Chunbiao L and Sprott J C 2013 Multistability in a butterfly flow *Int. J. Bifurcation Chaos* **23** 1350199

[50] Abdeljawad T and Baleanu D 2011 Fractional differences and integration by parts *J. Comput. Anal. Appl.* **13** 574–82

[51] Madalena C *et al* 2002 Multiscale entropy analysis of complex physiologic time series *Phys. Rev. Lett.* **89** 068102

[52] Shaobo H, Kehui S and Huihai W 2015 Complexity analysis and dsp implementation of the fractional-order lorenz hyperchaotic system *Entropy* **17** 8299–311

[53] Natiq H, Banerjee S and Ariffin M R K 2019 Can hyperchaotic maps with high complexity produce multistability? *Chaos* **29** 011103